Inorg. Chem. **2008**, *47*, 683–689

Synthesis and Thermal Chemistry of Copper (I) Guanidinates

Jason P. Coyle,[†] Wesley H. Monillas,[‡] Glenn P. A. Yap,[‡] and Seán T. Barry*[,†]

Department of Chemistry, Carleton University, 1125 Colonel By Drive, Ottawa, Ontario, Canada K1S 5B6, and Department of Chemistry and Biochemistry, University of Delaware, Newark, Delaware 19716

Received July 3, 2007

Copper (I) guanidinate dimers were generated by a salt metathesis route and structurally characterized. The guanidinates differed from the known amidinate dimers because of a large torsion of the dimer ring. This had a direct effect on their thermal chemistry. The thermal reactivity was investigated by several methods, including a novel temperature-resolved, gas-phase method that was monitored by mass spectrometry. The copper guanidinates underwent carbodiimide deinsertion to produce copper metal at temperatures between 225 –and 250 °C in the gas phase and at 125 °C in solution. The amidinate investigated also showed copper deposition at 190 °C in the gas phase, and 135 °C in solution, but without carbodiimide deinsertion. The guanidinate compounds deposited crystalline copper at 225 °C in a simple chemical vapor deposition experiment.

Introduction

Thin copper films are important in the advancement of microelectronic devices, and both chemical vapor deposition (CVD)[1] and atomic layer deposition (ALD)[2] are methods predicted to be used for copper interconnect production by the International Technology Roadmap for Semiconductors.[3] Organometallic copper precursors have been studied intensely as vaporous precursors for thin metal film deposition by ALD for this reason.[4] Among copper precursors, copper (I) compounds employing chelate ligands have shown tremendous utility in both CVD and ALD applications. Examples of these compounds include copper (I) and (II) β-diketonates,[5] copper (I) ketoiminates,[6] and β-diketimidates.[7]

Recently, copper (I) amidinate dimers have been reported as ALD precursors,[8] as well as being useful for investigating spin delocalization between copper metal centers.[9] These species exist as dimers wherein the amidinate ligand bridges two copper centers. We have extended this family of copper compounds to include copper (I) guanidinates. The exocyclic amido moiety will change the bonding mode of the ligand by permitting an additional resonance structure to exist for the compound (Scheme 1). When the ligand has an alkyl moiety in the exocyclic position (Scheme 1a), the π system is restricted to the dimer ring. When the exocyclic position is occupied by an amide, the π system can extend to the exocyclic nitrogen, permitting the imido resonance structure C (Scheme 1b). We were interested to see if this change in resonance, and its concomitant change in bonding within the dimer ring, would affect the thermal chemistry of the precursor.

* To whom correspondence should be addressed. E-mail: sbarry@ccs.carelton.ca.
† Carleton University.
‡ University of Delaware.

(1) Dopplet, P. *Coord. Chem. Rev.* **1998**, 1785.
(2) (a) Leskela, M.; Ritala, M. *Angew. Chem., Int. Ed.* **2003**, *42*, 5548. (b) Ritala, M.; Leskela, M. In *Handbook of Thin Film Materials*; Nalwa, H. S., Ed.; Atomic Layer Deposition, Chapter 2; Academic Press: San Diego, 2001; Vol. 1, p 103.
(3) 2005 Edition of the International Technology Roadmap for Semiconductors; http://www.itrs.net/Links/2005ITRS/Home2005.htm.
(4) (a) Kim, J. Y.; Kim, Y.-G.; Stickney, J. L. *J. Electrochem. Soc.* **2007**, *154*, 260. (b) Park, K.-H.; Bradley, A. Z.; Thompson, J. S.; Marshall, W. J. *Inorg. Chem.* **2006**, *45*, 8480. (c) Jezewski, C.; Lanford, W. A.; Wiegand, C. J.; Singh, J. P.; Wang, P. I.; Senkevich, J. J.; Lu, T. M. *J. Electrochem. Soc.* **2005**, *152*, 60. (d) Mane, A. U.; Shivashankar, S. A. *Mater. Sci. Semicond. Proc.* **2004**, *7*, 343. (e) Niskanen, A.; Rahtu, A.; Sajavaara, T.; Arstila, K.; Ritala, M.; Leskela, M. *J. Electrochem. Soc.* **2005**, *152*, 25.
(5) (a) Chen, T. Y.; Omnés, L.; Vaisserman, J.; Doppelt, P. *Inorg. Chim. Acta* **2004**, *357*, 1299. (b) Bollmann, D.; Merkel, R.; Klumpp, A. *Microelectron. Eng.* **1997**, *37*−*38*, 105. (c) Lagalante, A. F.; Hansen, B. N.; Bruno, T. J.; Sievers, R. E. *Inorg. Chem.* **1995**, *34*, 5781. (d) Wenzel, T. J.; Williams, E. J.; Haltiwanger, R. C.; Sievers, R. E. *Polyhedron* **1985**, *4*, 369.
(6) Lay, E.; Song, Y.-H.; Chiu, Y.-C.; Lin, Y.-M.; Chi, Y.; Carty, A. J. *Inorg. Chem.* **2005**, *44*, 7226.
(7) Park, K.-H.; Marshall, W. J. *J. Am. Chem. Soc.* **2005**, *127*, 9330.
(8) (a) Li, Z. W.; Rahtu, A.; Gordon, R. G. *J. Electrochem. Soc.* **2006**, *153*, 787. (b) Li, Z.; Barry, S. T.; Gordon, R. G. *Inorg. Chem.* **2005**, *44*, 1728. (c) Lim, B. S.; Rahtu, A.; Gordon, R. G. *Nat. Mater.* **2003**, *2*, 749. (d) Lim, B. S.; Rahtu, A.; Park, J.; Gordon, R. G. *Inorg. Chem.* **2003**, *42*, 7951.
(9) Jiang, X.; Bollinger, J. C.; Baik, M.-H.; Lee, D. *Chem. Commun.* **2005**, 1043.

10.1021/ic701317y CCC: $40.75
Published on Web 12/21/2007

Scheme 1. Resonance Structures for Copper Amidinate and Guanidinate Ligands

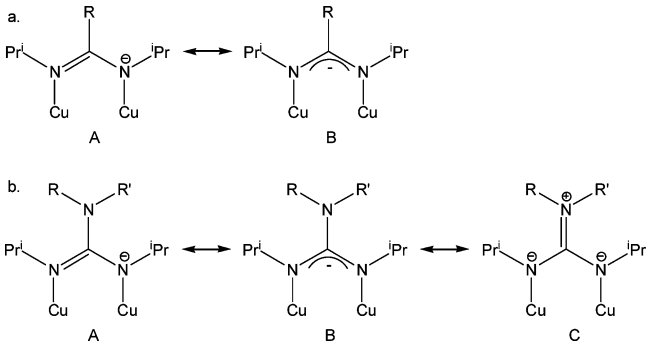

Scheme 2. Thermally Induced Carbodiimide Deinsertion

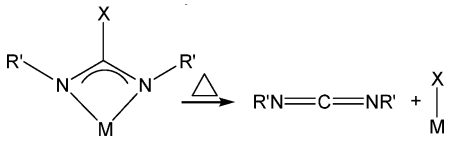

Specifically, our interest in copper guanidinate thermal chemistry is to determine as to whether carbodiimide deinsertion plays a role in its decomposition, as has been demonstrated in aluminum and gallium guanidinates (Scheme 2).[10−12]

We synthesized and structurally characterized two copper guanidinates and investigated their thermal reactivity through a number of experiments. Most significantly, we adapted a quadropole mass spectrometer to sample a thermolysis apparatus as the precursor vapor is passed through (see Experimental Procedures). By coupling the time-resolved sampling capacity of the spectrometer with the temperature ramp of the furnace, we were able to extract a temperature-resolved mass spectrum of vapor-phase species. This experiment allowed us to explore the thermal behavior of the precursors under the conditions they experience during a typical vapor deposition experiment. We also studied the thermolysis of the known amidinate $[MeC(^iPrN)_2Cu]_2$,[8d] to compare thermolysis between amidinates and guanidinates for copper. Finally, the new guanidinate compounds were shown to deposit crystalline copper films at 225 °C in a simple CVD experiment.

Results and Discussion

To determine the role of carbodiimide deinsertion on copper-containing systems, we synthesized and studied two copper (I) guanidinates: $[Me_2NC(^iPrN)_2Cu]_2$ (**1**) and $[^iPrN(H)C(^iPrN)_2Cu]_2$ (**2**). Both of these compounds were made at room temperature by salt metathesis

$$RC(^iPrN)_2Li + CuCl \rightarrow 1/2\,[RC(^iPrN)_2Cu]_2 + LiCl$$

where R = Me_2N (**1**) and $^iPrN(H)$ (**2**). These compounds formed in excellent yields (96% **1** and 89% **2**), and the simplicity of their ^1H NMR spectra suggested a symmetrical structure in both cases. Single X-ray quality crystals for both **1** and **2** were grown from Et_2O, and their structures were determined (Figure 1and Tables 1and 2).

Both compounds have a C_2 axis perpendicular to the Cu−Cu axis. The C_2 axis in **1** is parallel to the mean plane of the N atoms; in **2**, it is perpendicular to the nitrogen atom plane. The Cu−N bond lengths for both compounds are within the range of 1.87−1.88 Å, which agrees well with copper amidinates that have the same dimeric structure.[8,9] The Cu−Cu distances in **1** and **2** were 2.42 and 2.43 Å, respectively. This falls within the range of general Cu−Cu bonds with bridging ligands and is much shorter than the Cu−Cu distance in metallic copper.[13] These are intermediate to the reported copper distances in the amidinate dimers (2.40 Å (ref 8) and 2.46 Å (ref 9)). The C−N−C angles are also similar (120.0° for **1** and 120.5° for **2**, as compared to 119.6° (ref 8) for **1** and 120.1° (ref 9) for **2**).

The guanidinate compounds' structures differ in that the ligand−copper plane is noticeably twisted, and this can be highlighted by considering the N1−N1A−N3−N3A torsion angle (32.0° for **1** and 37.5° for **2**; Figure 2), while previously reported amidinates are much more planar (2.0° (ref 8) and 0° (ref 9)).

This core twist can be attributed to the participation of the exocyclic amido moiety of the guanidinates participating in the π system of the chelate ring, effectively allowing the amides to be slightly pyramidalized (Scheme 1b, structure C). This is common for guanidinate ligands.[11]

Thermolysis

The guanidinate compounds were studied to determine their thermal chemistry and compared to the previously reported $[MeC(^iPrN)_2Cu]_2$ (**3**).[8] The thermolysis study was performed in three stages.

Initially, thermogravimetric analyses were collected for each compound to determine their volatility (Figure 3and Table 3). All three compounds showed very similar volatilization, even though their melting points differed significantly. This is also reflected in the onset of volatilization of the compounds, which did not follow the melting point trend. As well, each compound showed a very low residual mass (<5% in all cases). These experiments suggest that all three precursors would be equally good copper precursors and might lead one to assume that their deposition and thermal decomposition chemistries were similar. However, further thermolysis studies revealed that the thermal chemistry of the copper guanidinates differed significantly from that of the copper amidinate.

Each compound was subjected to a sealed tube thermolysis, wherein a sealed, heavy walled NMR tube was heated in a tube furnace at intervals from room temperature to a maximum of 235 °C. Periodically, ^1H NMR spectra were collected to determine what, if any, thermolysis products

(10) Rowley, C. N.; DiLabio, G. A.; Barry, S. T. *Inorg. Chem.* **2005**, *44*, 1983.
(11) Kenney, A. P.; Yap, G. P. A.; Richeson, D. S.; Barry, S. T. *Inorg. Chem.* **2005**, *44*, 2926.
(12) Brazeau, A. L.; Wang, Z.; Rowley, C. N.; Barry, S. T. *Inorg. Chem.* **2006**, *45*, 2276.
(13) Cotton, F. A.; Wilkinson, G; Murillo, C. A; Bochmann, M. *Advanced Inorganic Chemistry*, 6th ed.; Wiley-Interscience: New York, 1999; p 861.

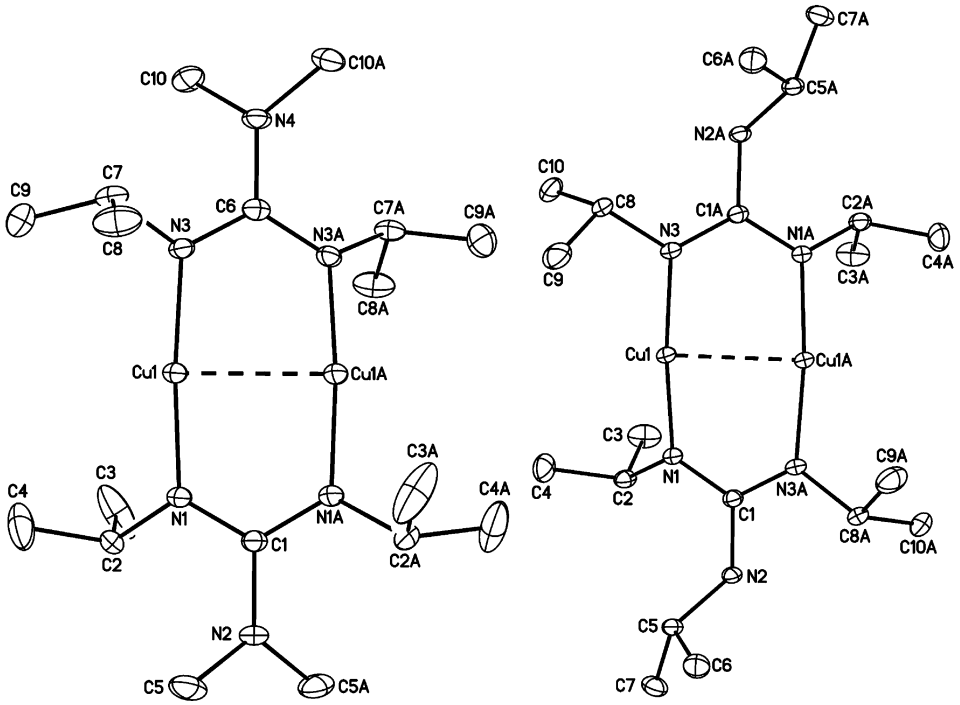

Figure 1. Single-crystal X-ray structures for **1** and **2**. Hydrogen atoms were omitted for clarity, and the thermal ellipses are shown at 30%.

Table 1. Selected Crystal Data and Structure Refinement Parameters

	$C_{18}H_{40}Cu_2N_6$ (**1**)	$C_{20}H_{44}Cu_2N_6$ (**2**)
fw	467.64	495.69
T (K)	120	120
λ (Å)	0.71073	0.71073
cryst syst	orthorhombic	monoclinic
space group	$C222_1$	$C2/c$
a (Å)	11.329	23.939
b (Å)	21.308	5.943
c (Å)	9.923	21.238
α (deg)	90.00	90.00
β (deg)	90.00	122.45
γ (deg)	90.00	90.00
V (Å^3)	2395	2550
Z	4	4
ρ_{calcd} (mg/m^3)	1.297	1.291
abs coeff (mm^{-1})	1.788	1.684
refinement method	full-matrix least-squares on F^2	full-matrix least-squares on F^2
R indices [$I > 2\sigma(I)$][a]	R1 = 0.0360, wR2 = 0.0860	R1 = 0.0440, wR2 = 0.1068

[a] $R1 = \sum||F_o| - |F_c||/\sum|F_o|$ and $wR2 = (\sum w(|F_o| - |F_c|)^2/\sum w|F_o|^2)^{1/2}$.

were identifiable. For **1** and **2**, characteristic ^{1}H NMR peaks for diisopropylcarbodiimide (CDI), as well as dimethylamine for **1** and isopropylamine for **2**, were seen at 135 °C and subsequently increased in intensity at higher temperatures. Deinsertion of CDI from guanidinate ligands is a prevalent thermolysis route.[11,12] Additional support for this thermolysis route was seen by FT-IR spectroscopy. For both **1** and **2**, FT-IR analysis of the solution resulting from the NMR tube thermolysis showed an absorbance at 2120 cm^{-1}, which is indicative of the asymmetric stretch of CDI. Very tellingly, the copper metal plated out of solution and deposited on the walls of the NMR tube in both cases, showing that (in solution, at least) **1** and **2** are viable precursors for copper metal without requiring a reducing agent.

The most likely decomposition mechanism for these guanidinates is the deinsertion of carbodiimide. This deinsertion is followed by decomposition of the resulting copper (I) amide through deprotonation of the amide by another amide to produce an imide (Scheme 3). This reactivity has been seen previously by Saegusa et al.[14] Peaks in the FT-IR spectra of the thermolysis solution also support this reaction scheme. The FT-IR spectra showed a peak at 1639 cm^{-1} for both **1** and **2** that is attributed to the imides resulting from copper amide deprotonation. The corresponding amines were not seen in the IR, but we speculate that they evaporated during the IR plate preparation.

We were interested to see if CDI deinsertion was occurring in the vapor phase for the guanidinate compounds and whether the amidinate species would show any CDI deinsertion at elevated temperatures. Using a furnace coupled to a quadrapole mass spectrometer, we able to collect temperature-resolved mass spectra. This experiment is much more

(14) Tsuda, T.; Wantanabe, K.; Miyata, K.; Yamamoto, H.; Saegusa, T. *Inorg. Chem.* **1981**, *20*, 2728.

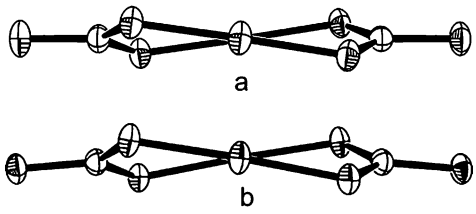

Figure 2. Dimer cores of (a) **1** and (b) **2**, showing the twists induced by pyramidalization of the chelating nitrogens. Except for the ligands' sp^2 carbon, all carbon and hydrogen atoms are omitted for clarity, and the thermal ellipses are shown at 30%.

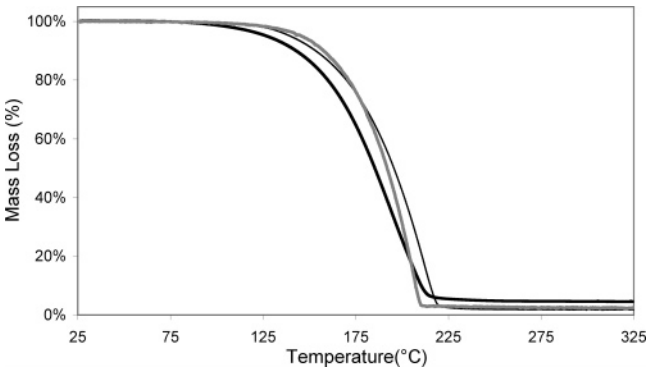

Figure 3. Thermogravimetric analyses of **1** (solid line), **2** (bold line), and **3** (gray line).

Table 2. Selected Bond Lengths and Angles for **1** and **2**

1		**2**	
	Selected Bond Lengths (Å)		
Cu1−N1	1.875(2)	Cu1−N1	1.875(2)
Cu1−N3	1.876(2)	Cu1−N3	1.871(2)
Cu1−Cu1A	2.4233(10)	Cu1−Cu1A	2.4289(11)
N1−C1	1.341(3)	N1−C1	1.338(3)
N3−C6	1.334(3)	N3−C1	1.345(3)
N2−C1	1.396(5)	N2−C1	1.399(3)
N4−C6	1.411(5)		
	Selected Bond Angles (deg)		
N1−Cu1−N3	174.75(10)	N1−Cu1−N3	173.71(8)
C7−N3−Cu1	117.14(18)	C8−N3−Cu1	121.38(15)
C2−N1−Cu1	118.66(18)	C2−N1−Cu1	117.93(13)
N3−C6−N3A	120.4(3)	N1−C1−N3A	120.51(19)
N1−C1−N1A	120.4(3)		
	Sum of Angles (deg)		
N1	358.2	N1	357.8
N3	357.3	N3	360
N2	360	C1	359.9
N4	360		
C1	360		
C6	360		
	Torsion Angles (deg)		
N1−N1A−N3−N3A	32	N1−N3A−N3−N1A	37.5

indicative of the environment that the precursors would be subjected to in a CVD or ALD experiment: the precursors are thermolyzed at low concentration in the gas phase and exposed to the thermolysis zone for a relatively short period of time. Thus, we anticipated that the thermolysis chemistry would correlate to the TGA, as well as the solution thermolysis, but the reaction temperatures would not correspond exactly to the vapor-phase experiments.

For **1**, a mass signal for the free guanidine (171 amu) was seen to decrease significantly at 225 °C, with a corresponding increase in the mass signal for carbodiimide (126 amu) (Figure 4). This trend is also apparent in ionization fragments

Table 3. Thermal Decomposition Data for **1**−**3**

	1	**2**	**3**
melting point (°C)	110	79	147
onset of volatilization[a] (°C)	105	87	102
TGA residual mass (%)	1.8	4.6	2.2
initial copper deposition, NMR tube (°C)	125	125	135
onset of deinsertion, NMR tube (°C)	135	135	
onset of deinsertion, tube furnace (°C)	225	250	

[a] Onset of volatilization is considered to be the point in the TGA where 1% of the mass is lost.

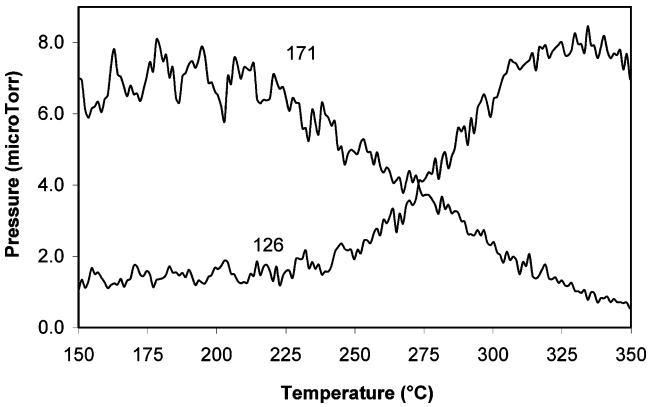

Figure 4. Temperature-resolved mass spectrum of **1** showing the increase in carbodiimide and a corresponding decrease in the dimethylamido diisopropyl guanidine.

Scheme 3. Thermal Decomposition of Copper Guanidinates

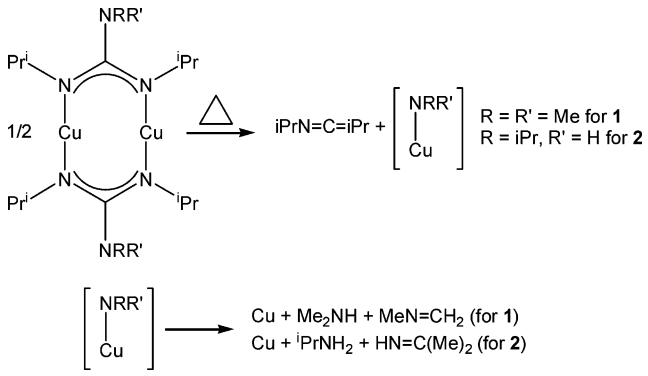

of the carbodiimide, notably mass 111 amu (CDI-Me). This suggested that at temperatures below 225 °C, the whole precursor is surviving to reach the mass spectrometer, and fragmentation in the mass spectrometer produces the guanidine ion. At 225 °C, CDI begins to thermally deinsert while the precursor is in the tube furnace, and thus, it and its fragments become prominent in the mass spectrum above this temperature. It should be noted that the CDI is seen to diminish above about 300 °C, where diisopropyl carbodiimide itself undergoes thermal decomposition.

Although this temperature was greater than the 125−135 °C measured in the sealed tube thermolysis, this is likely a kinetic effect due to the low residence time of the precursor in the thermolysis zone during the vapor-phase experiment. This is a good indication that this species could be used for ALD deposition below 225 °C, as thermal decomposition precludes ALD deposition. Above 225 °C, this species might be used as a CVD precursor for copper metal without requiring a reducing agent.

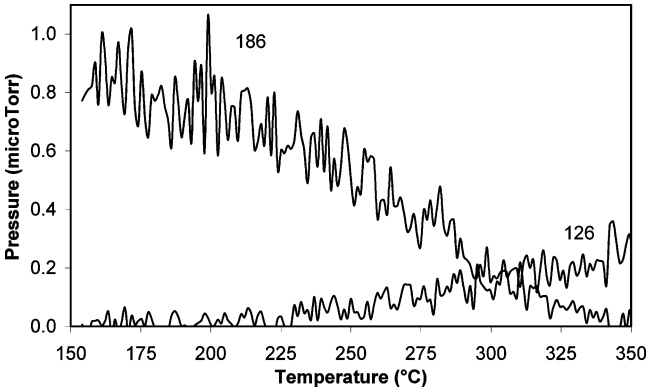

Figure 5. Temperature-resolved mass spectrum of **2** showing the increase in carbodiimide and a corresponding decrease in the protonated triisopropyl guanidine cation.

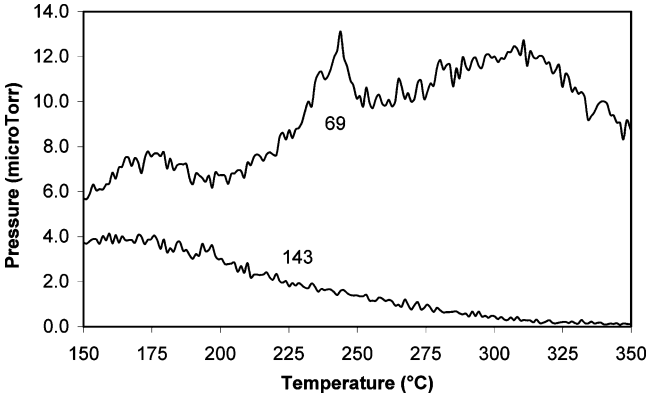

Figure 6. Temperature-resolved mass spectrum of **3** showing the increase in the ligand fragment C═N^{i}Pr and a corresponding decrease in the protonated acetamidine cation.

For **2**, the mass signal for the protonated guanidine cation (186 amu) was seen to decrease significantly at 200 °C (Figure 5). The fragments of this species also echoed this trend. At the same time, the mass signal for CDI (126 amu) started to ramp in very slowly at approximately 225 °C. The fragments of this species follow this trend and were again most obvious for the mass 111 amu. This again suggested that the whole precursor is surviving to reach the mass spectrometer until temperatures higher than 225 °C, where deinsertion begins to play a significant role, similar to **1**. Interestingly, the amidinate **3** gave very different thermal behavior, even though its thermal chemistry occurred at similar temperatures (Figure 3 and Table 3).

The NMR tube thermolysis experiment showed no characteristic isopropyl signals for CDI in the ^{1}H NMR, even up to 235 °C, the practical limit of this thermolysis experiment. Additionally, there was no evidence of carbodiimide in solution FT-IR. However, copper metal was seen to deposit on the walls of the NMR tube at 135 °C.

The ^{1}H NMR showed no new signals until 235 °C where peaks corresponding to the amidine ligand appeared. Further thermolysis experiments in a sealed pressure vessel at 235 °C allowed the isolation of a small amount of air-sensitive, colorless oil as well as deposited metallic copper. This oil tested positive for copper using a qualitative flame test, and a GC-MS of the oil showed a single peak at 143 amu, which corresponds with the mass of the protonated amidine ligand.

Although unambiguous characterization of this oil was not achieved due to its extreme reactivity and very low isolated mass, we suspect that this might be a paramagnetic homoleptic copper (II) diisopropyl acetamidinate, liberated through disproportionation of the copper (I) precursor

$$[\mathrm{MeC}(^i\mathrm{PrN})_2\mathrm{Cu}]_2 \rightarrow \mathrm{Cu}(0) + (\mathrm{MeC}(^i\mathrm{PrN})_2)_2\mathrm{Cu}$$

We suspect that further thermolysis of the copper (II) acetamidinate leads to a protonated amidine ligand by an unknown decomposition pathway. Similar reactivity has recently been reported for copper (I) betadiketiminates[15] as well as previously in copper (I) betadiketonate chemistry.[16] This reactivity needs to be further disambiguated and is a topic of research in our laboratory.

Compound **3** also showed no evidence of carbodiimide deinsertion in the temperature-resolved MS, to the maximum temperature of this experiment. The characteristic parent and fragment mass signals at 126 and 111 amu remained undetectably close to zero throughout the temperature range. However, a mass signal for the parent guanidine cation peak (143 amu) started to decline at about 190 °C with a corresponding increase in the mass signal for the fragment ^{i}Pr−N═C (69 amu) (Figure 6). This suggests that the main thermal decomposition pathway for the amidinate is not by CDI deinsertion but by destruction of the amidinate itself. Unfortunately, the vapor-phase thermolysis experiment could not identify the potential copper (II) amidinate from disproportionation, as the mass of this species is above the limit of the mass spectrometer.

Simple CVD experiments were undertaken to demonstrate the utility of **1** and **2** as precursors. The depositions were performed in a tube furnace at 225 °C under roughing pump vacuum ($\sim 10^{-3}$ Torr). A nitrogen carrier gas was used (20 sccm), and this was pulsed on and off at 3 s intervals. The pulsing was necessary to promote volatilization of the copper precursor due to the design of the reactor. Silicon (111) with a native oxide coating was used as a substrate.

Both guanidinate precursors produced metallic, copper-colored films. Scanning electron micrographs showed the films to be microparticulate to nanoparticulate, which is commonly the case with vapor-deposited copper (Figure 7).[17] X-ray diffraction identified the films as polycrystalline copper in both cases (Figure 8), and energy dispersive X-ray analysis corroborated this fact. The growth is quite different in each case, with **2** showing a much larger crystallite formation and a wide variety of shapes. The film grown by **1** consisted mainly of >100 nm crystallites with a faceted boulder appearance, while the film grown from **2** showed boulders up to 500 nm, as well as rods, some as long as 2 μm.

(15) Shimokawa, C.; Tachi, Y.; Nishiwaki, N.; Ariga, M.; Itoh, S. *Bull. Chem. Soc. Jpn.* **2006**, *79*, 118.

(16) (a) Chen, T.-Y.; Vaissermann, J.; Ruiz, E.; Sénateur, J. P.; Doppelt, P. *Chem. Mater.* **2001**, *13*, 3993. (b) Chi, K. M.; Shin, H.-K.; Hampden-Smith, M. J.; Duesler, E. N. *Polyhedron* **1991**, *19*, 2293.

(17) Kaloyeros, A. E.; Eisenbraun, E. *Annu. Rev. Mater. Sci.* **2000**, *30*, 363.

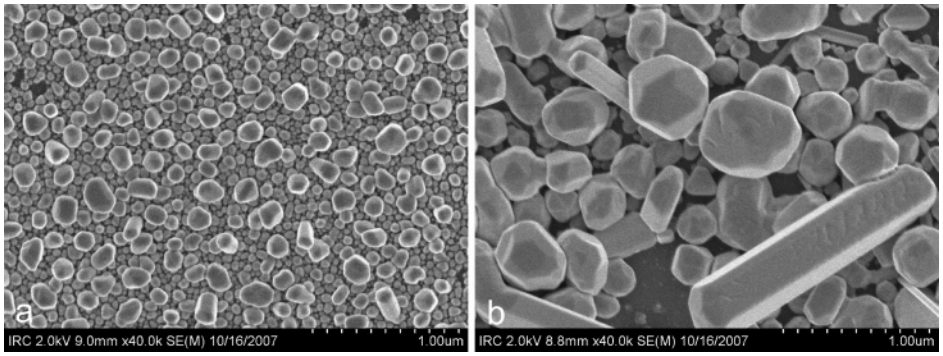

Figure 7. Scanning electron micrograph of copper films deposited by (a) **1** and (b) **2**.

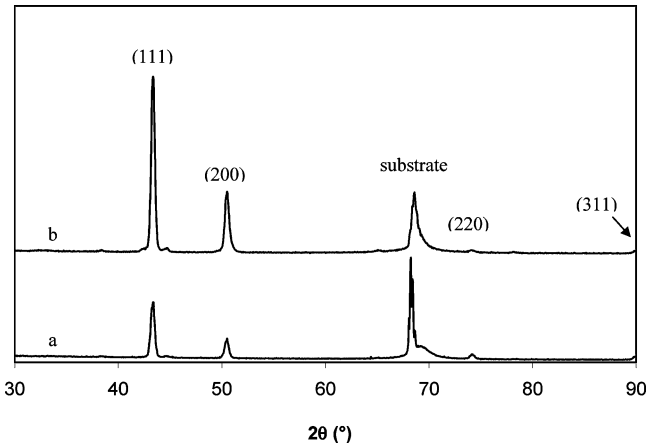

Figure 8. X-ray diffraction spectra of copper deposited in a CVD experiment using (a) **1** and (b) **2** as a precursor.

The mass spectrometer data for each compound supported the decomposition pathway suggested in Scheme 3. The mass spectra showed parent peaks for the guanidinate ligands, as well as for CDI and its fragmentation products. The partial pressure for CDI was higher then that of the parent guanidinate ligands, which is a sign of deinsertion occurring before fragmentation in the mass spectrometer. Ideally, deposition of copper by a CDI deinsertion decomposition pathway would show only CDI as a significant peak in the in situ QMS data; however, a partial pressure of the guanidinate ligand was detectable during deposition. This was not surprising considering that the vaporous precursor is unlikely to be totally consumed by deposition. In the case of **1**, a fragment with a mass of 44 amu was abundant in the mass spectrum, registering as high as 2×10^{-4} Torr, which was a very high partial pressure as compared to other mass channels. This could be attributed to the protonated form of the fragment $MeN{=}CH_2$, as speculated in Scheme 3. Similarly for **2**, a fragment with a mass of 58 amu showed a partial pressure of 2×10^{-5} Torr and was attributed to the protonated form of the fragment $HN{=}CMe_2$ (Scheme 3). It should be noted that these masses are common fragments of their respective ligands, and thus, we are presently studying this thermal decomposition pathway more closely to verify our suggested mechanism.

Conclusion

The copper (I) guanidinate compounds show a similar response to temperature as copper (I) amidinate: they deposit copper metal at temperatures just above 100 °C in a sealed tube experiment. However, the guanidinates do so through a carbodiimide deinsertion reaction, while the amidinate undergoes a more complicated thermolysis, potentially involving the disproportionation of copper (I) to produce metallic copper and copper (II). Temperature-resolved mass spectrometry showed that the thermolysis of both the amidinate and the guanidinates decomposed at higher temperatures in the dilute gas phase, albeit by mechanisms that were similar to their respective sealed-tube experiments. We attribute the higher decomposition temperature in the gas-phase experiment to the short exposure time of the precursor to an elevated temperature. This better emulates the conditions these species would encounter during a typical ALD experiment and thus allows the determination of the temperature limit for these species as ALD precursors. Finally, both **1** and **2** showed deposition of copper metal at 225 °C without a secondary gas, demonstrating their utility as CVD precursors for copper metal films.

Experimental Procedures

Synthesis. All manipulations were carried out in an MBraun Unilab inert atmosphere drybox. $Li(^iPrN)_2CN(H)^iPr$ was synthesized following literature preparation for general guanidinate synthesis.[18] Lithium dimethyl amide, diisopropyl carbodiimide, and copper (I) chloride were purchased from Aldrich Chemical Co. and used as received. Hexanes and diethyl ether were purified with respect to oxygen and water using an MBraun solvent purification system and stored on activated 4A sieves until used. Guelph Chemical Laboratories in Guelph, ON, Canada, performed combustion analyses.

$[Me_2NC(^iPrN)_2Cu]_2$ (1). In a 50 mL flask, $LiNMe_2$ (0.274 g, 5.10 mmol) was suspended in 30 mL of hexanes. Diisopropylcarbodiimide (0.668 g, 5.30 mmol) was diluted in 8 mL of hexanes and added dropwise to the suspension of $LiNMe_2$. The cloudy, pale yellow suspension cleared to a homogeneous pale yellow solution over 2 h of stirring. CuCl (0.521 g, 5.10 mmol) was added, and the mixture was stirred for 18 h, after which a cloudy light green solution was filtered to afford a light green solid and a slightly pale yellow solution. Volatiles were removed under reduced pressure to afford a crystalline off-white solid (1.14 g, 95.9% crude yield). The solid was dissolved in a minimal volume of diethyl ether and was kept at −30 °C overnight. Compound **1** was collected as clear, colorless crystals (0.86 g, 72%). mp 109 °C. Anal. calcd

(18) Foley, S. R.; Yap, G. P. A.; Richeson, D. S. *Chem. Commun.* **2000**, 1515 and references therein.

for $C_{18}H_{40}Cu_2N_6$: C, 46.23; H, 8.62; N, 17.97. Found: C, 46.51; H, 9.01; N, 18.22 Mass spectra *m*/*e* (relative abundance): 466 (0.1) M^+. ^{1}H NMR (300 MHz, C_6D_6: δ 3.41 [sept, 4H, NC*H*^{i}Pr], δ 2.54 [s, 12H, N(CH_3)$_2$], δ 1.29 [d, 24H NCH(CH_3)$_2$]. ^{13}C NMR (75 MHz, C_6D_6): δ 48.22 [*C*HCH$_3$], δ 27.59 [CH*C*H$_3$], δ 40.92 [N(*C*H$_3$)$_2$, δ 171.58 [(^{i}PrN)$_2$CNMe$_2$].

[^{i}PrN(H)C(^{i}PrN)$_2$Cu]$_2$ (2). In a 250 mL flask, Li(^{i}PrN)$_2$CN(H)^{i}Pr (7.727 g, 40.4 mmol) was added to a suspension of CuCl (4.0 g, 40.4 mmol) in 100 mL of hexanes. The solution was stirred for 18 h. It was filtered to afford a pale yellow, clear solution. Volatiles were removed under reduced pressure to yield **2** as an off-white crystalline mass (8.9 g, 89%). The crude product was recrystallized from 10 mL of diethyl ether to afford clear, colorless crystals, (6.69 g, 67%). mp 79 °C. Anal. calcd for $C_{18}H_{40}Cu_2N_6$: C, 48.46; H, 8.95; N, 16.95. Found: C, 48.36; H, 9.17; N, 16.58 Mass spectra *m*/*e* (relative abundance): 494 (0.1) M^+. ^{1}H NMR (300 MHz, C_6D_6: δ 3.64 [sept, 4H, NC*H*Me$_2$], δ 3.46 [sept, 2H, HNC*H*Me$_2$], δ 3.06 [d, 2H *H*NCHMe$_2$], δ 1.30 [d, 24H NCH(CH_3)$_2$], δ 0.97 [d, 12H HNCH(CH_3)$_2$]. ^{13}C NMR (75 MHz, C_6D_6): δ 27.67 [NCH*C*H$_3$], δ 47.49 [N*C*HCH$_3$], δ 23.55 [HNCH(*C*H$_3$)$_2$, δ 48.44 [HN*C*H(*C*H$_3$)$_2$, δ 171.58 [(^{i}PrN)$_2$CNMe$_2$].

Crystallography. Crystals were selected and mounted on plastic loops with viscous oil and cooled to the data collection temperature. Diffraction data were collected on a Bruker-AXS APEX CCD diffractometer. All data sets were treated with SADABS absorption corrections. Unit cell parameters were determined by sampling three different sections of the Ewald sphere. The systematic absences in the diffraction data were consistent for *Cc* and *C*2/*c* for **2** and, uniquely, for *C*222$_1$ for **1**. Structural solution in the centrosymmetric space group option for **2** yielded chemically reasonable and computationally stable results of refinement. The anomalous dispersion factor was refined to zero in **1**, indicating that the true hand of the data was determined. The compound molecules were located on two-fold symmetry. All non-hydrogen atoms were refined with anisotropic displacement parameters. All hydrogen atoms were treated as idealized contributions. Structure factors are contained in the SHELXTL 6.12 program library.[19]

Sealed NMR Tube Thermolysis. NMR samples of **1**−**3** were prepared in thick-walled NMR tubes using C_6D_6 as solvent. The tubes were sealed while frozen in liquid nitrogen and under reduced pressure. The three samples were left overnight in a furnace at the following temperatures: 100, 125, 135, 150, 175, 190, 205, 225, and 235 °C. After each thermolysis, a ^{1}H NMR spectrum was collected.

Gas-Phase Thermolysis (TGA). A bubbler was charged with the compound of interest and heated to 5 °C above the compound's melting point to increase the vapor pressure. This was coupled through a high-vacuum fitting to our homemade ALD reactor, which was run with all of its valves open and with no carrier gas. The vapor was carried through a tube furnace that was ramped from 150 to 450 °C at 3°/min. The resulting gas-phase species were sampled by a Microvision Plus 1000e "SmartHead" 300 amu quadropole mass spectrometer, thus allowing a temperature-resolved, gas-phase thermolysis experiment to be carried out.

Acknowledgment. This work was supported by an NSERC discovery grant to S.T.B. Thanks to Jim Margeson at NRC-IMS (Ottawa) for FE-SEM images and Mostofa Kamal at Carleton University for XRD data.

Supporting Information Available: CIF files for **1** and **2**. This material is available free of charge via the Internet at http://pubs.acs.org.

IC701317Y

(19) Sheldrick, G. M. *SHELXTL 6.12*; Siemens XRD: Madison, WI, 2001.